

Dynamic Friction Unraveled by Observing an Unexpected Intermediate State in Controlled Molecular Manipulation

Norio Okabayashi^{1,*}, Thomas Frederiksen^{2,3,†}, Alexander Liebig⁴, and Franz J. Giessibl^{4,‡}

¹*Graduate School of Natural Science and Technology, Kanazawa University, Ishikawa 920-1192, Japan*

²*Donostia International Physics Center (DIPC), San Sebastián 20018, Spain*

³*IKERBASQUE, Basque Foundation for Science, Bilbao 48013, Spain*

⁴*Institute of Experimental and Applied Physics, University of Regensburg, Regensburg D-93053, Germany*

 (Received 7 January 2023; revised 26 April 2023; accepted 30 August 2023; published 2 October 2023)

The pervasive phenomenon of friction has been studied at the nanoscale via a controlled manipulation of single atoms and molecules with a metallic tip, which enabled a precise determination of the static friction force necessary to initiate motion. However, little is known about the atomic dynamics during manipulation. Here, we reveal the complete manipulation process of a CO molecule on a Cu(110) surface at low temperatures using a combination of noncontact atomic force microscopy and density functional theory simulations. We found that an intermediate state, inaccessible for the far-tip position, is enabled in the reaction pathway for the close-tip position, which is crucial to understanding the manipulation process, including dynamic friction. Our results show how friction forces can be controlled and optimized, facilitating new fundamental insights for tribology.

DOI: 10.1103/PhysRevLett.131.148001

The atomic origin of friction is complex because it arises from the interplay of several physical mechanisms typically spanning diverse length scales [1–4]. Seeking to isolate these mechanisms, research on friction has reached the atomic level in the past decades owing to the advancements in experimental techniques, such as scanning tunneling microscopy (STM) and atomic force microscopy (AFM) [5,6], and computer simulation capabilities. Indeed, the empirical laws observed at the macroscopic scale have been linked to the processes at nanoscale [7–14]. The most elementary approach to study friction would be to observe a single atom moving over a surface using STM and AFM [15–23]. These techniques are primarily used to visualize single atoms and molecules on surfaces, and even allow their manipulation through the interaction force from the tip, enabling the fabrication of fascinating structures, such as quantum corrals [24], computing devices [25], and molecular graphene [26]. A remarkable outcome of the manipulation research is the measurement of the lateral force needed to initiate sliding of single atoms [19,21,22], i.e., the determination of the static friction force. However, obtaining insights into dynamic friction (force needed to continue sliding) at the atomic scale requires a complete picture of the dynamics, including the intermediate states and energy dissipation, which is missing so far. Here, we address this challenge by revealing the dynamics during manipulation on a Cu(110) surface of a CO molecule, which is probably the most widely studied molecule in the field of surface science [27].

All measurements were performed at 4.4 K under ultrahigh vacuum conditions using a combined STM and AFM system. A Cu(110) crystal was cleaned by repeated

sputtering and annealing, on which CO molecules were adsorbed. The force field was measured using a qPlus sensor [28] with the eigenfrequency $f_0 = 52\,194$ Hz, stiffness $k = 1800$ N/m, and quality factor $Q = 595\,000$, in which a metallic tip was attached to the cantilever end. The frequency shift Δf of the vertically oscillating sensor due to the interaction force was measured at a constant amplitude $A = 20$ pm and zero bias, which was then converted into a potential energy [29]. During the Δf measurement, the excitation voltage V_{exc} to mechanically oscillate the cantilever at a constant amplitude was simultaneously measured, which was used to estimate the dissipation energy E_{dis} per oscillation cycle, using the following equation: $E_{\text{dis}} = 2\pi k A^2 / (2Q) \times V_{\text{exc}} / V_{\text{exc}0}$ [28], where $V_{\text{exc}0}$ is the excitation voltage when the tip is far away. We also computed the potential energy landscape and forces using periodic, plane-wave density functional theory as implemented in VASP [30] using the vdW-DF2 functional [31]. Calculations were performed with the plane-wave energy cutoff set to 600 eV, a 4×4 Monkhorst-Pack k -point mesh, and first-order Methfessel-Paxton occupations with 0.1 eV smearing. The CO-Cu(110) system was represented in a 2×3 surface unit cell slab with 8 atomic layers and ~ 2 nm vacuum region between periodic images. A Cu₁₁ cluster was explored as a model tip apex geometry. For each fixed tip position, geometry relaxation of CO and topmost 12 Cu surface atoms was performed with a force tolerance of 10^{-4} eV/pm. Background subtraction of the interaction energy was performed by evaluating also the total energy for supercells without CO. The nudged elastic band method [32] was used to

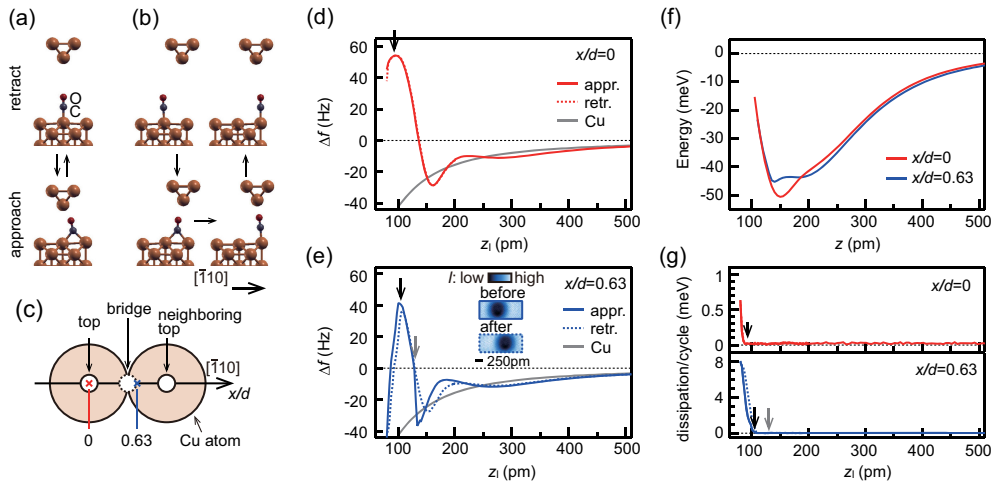


FIG. 1. (a) Schematic of CO manipulation on Cu(110) between top and bridge sites by a metallic tip over the top site. The thin arrows indicate the reaction processes of CO for tip approach and retract. (b) Same as (a), but for CO manipulation from top to neighboring top site when the tip approach and retract occurs for a tip position laterally closer to the neighboring top site. (c) Definition of lateral tip positions along Cu $\bar{1}10$ ($d = 255$ pm): $x/d = 0$ (top site) and $x/d = 0.63$ (outside of bridge). (d) Measured frequency shift (Δf) as a function of vertical tip position (z_1) for the tip-on-top-site case ($x/d = 0$). The Δf curves for tip approach and retraction are depicted by red solid and dotted lines, respectively. The Δf curve for the tip on Cu is also depicted by a gray line. (e) Same as (d), but for the lateral tip position $x/d = 0.63$ (outside of bridge). In the inset, typical STM images of CO before and after the manipulation are shown. (f) Measured potential energy between the tip and CO up to the point of manipulation. (g) Energy dissipation per cycle of the vertically oscillating tip, where both cases of tip approach and retract are depicted.

compute reaction pathways. Additional experimental and theoretical details are described in [33,34].

CO manipulation by vertical tip motion.—Figures 1(a) and 1(b) summarize two manipulation scenarios, deduced from our density functional theory calculations detailed below, using selected geometries here for visualization purposes. When the tip is located far from the substrate, CO adsorbs on a top site in an upright configuration with its C atom bound to the Cu atom [Fig. 1(a), top]. When the tip apex is centered over the top site and brought sufficiently close to the substrate, CO moves along the $\bar{1}10$ direction to a bridge site [Fig. 1(a), bottom]. Consequently, bringing a vertically oscillating tip close to the surface directly over the CO molecule, correlated lateral jumps of CO between the top and bridge sites are induced. When a tip approaches on a laterally shifted location closer to one of the neighboring top sites, CO is first manipulated to jump from the top to neighboring top via bridge site [Fig. 1(b)]. If the tip retracts from this height, CO irreversibly ends up in this neighboring top site.

To investigate these two manipulation processes, i.e., reversible top \leftrightarrow bridge and irreversible top \rightarrow bridge \rightarrow neighboring-top CO motion, we measured the frequency shift (Δf) of the vertically oscillating force sensor, with a metallic tip, as a function of its height (z_1) at various lateral tip positions [34]. Two exemplary cases [Fig. 1(c)] of the lateral tip positions (x) are shown in Figs. 1(d) and 1(e): tip on top site ($x/d = 0$) and tip closer to the neighboring top site ($x/d = 0.63$), where d is the distance between the nearest neighboring Cu atoms (255 pm). As shown in

Fig. 1(d), when the tip over the top site approaches CO, Δf first decreases until $z_1 = 160$ pm and then increases. When the tip approaches beyond $z_1 = 93$ pm (black arrow), Δf decreases abruptly, indicating that the CO molecule has moved away from the top site.

Similar abrupt decreases in Δf are also observed for the lateral tip positions inside the bridge side [34]. For these cases, the Δf curves for tip retraction and approach are identical as shown in Fig. 1(d); the CO molecule is adsorbed on the initial top site after the retraction. However, with the tip positioned beyond the bridge site [Fig. 1(e)], a discontinuous change in Δf at $z_1 = 131$ pm (gray arrow) is observed for the tip-approach case. In addition, the Δf curve for tip retraction is different from that for tip approach when $z_1 > 131$ pm. After the tip retraction, we confirmed that the CO had moved to the neighboring top site that corresponds to $x/d = 1$, as shown in the inset. These observations indicate that the discontinuous change in the Δf curve in the approaching direction is caused by a lateral movement of CO to the neighboring top site, whereas a reverse manipulation does not occur during the retraction [Fig. 1(b)]. Note that once the manipulation to the neighboring top site occurs, the situation becomes similar to the case of Fig. 1(a) and 1(d). Indeed, for approaching the tip further to $z_1 = 105$ pm, Δf decreases abruptly as shown by the black arrow.

Figure 1(f) shows the potential energy between tip and CO until the manipulation between top and bridge occurs for $x/d = 0$ (red) and until the manipulation to the neighboring top site occurs for $x/d = 0.63$ (blue). For

both cases, the manipulation occurs at a tip height that is lower than the value for the potential minimum, indicating that the manipulation takes place in the repulsive force regime. Moreover, when an abrupt decrease in Δf is observed ($z_1 = 93$ pm for $x/d = 0$ and $z_1 = 105$ pm for $x/d = 0.63$), a noticeable energy dissipation occurs as shown by the black arrows in Fig. 1(g). In contrast, no increase in energy dissipation is observed when the CO molecule is manipulated to the neighboring top site for $x/d = 0.63$ at $z_1 = 131$ pm (gray arrow).

Energy dissipation during vertical tip oscillation.—To understand the energy dissipation that occurs during these manipulation processes, we calculated the potential energy between model tip structures and a CO molecule on Cu(110) as a function of lateral and vertical tip position (x and z_{cal}) [34]. Two exemplary cases of the lateral tip position for a relatively inert tip structure comprising 11 Cu atoms are shown in Figs. 2(a) and 2(b), where $x/d = 0.3$ (inside of bridge) and 0.8 (outside of bridge). When the tip is positioned laterally near the top site where the CO is initially adsorbed [Fig. 2(a)], the crossover to molecular adsorption in the bridge configuration is energetically preferred in the repulsive force regime, consistent with the experimental observations [Fig. 1(f)]. This scenario was further confirmed using inelastic electron tunneling spectroscopy [34].

To reveal the origin of the energy dissipation, we analyzed the potential energy along the reaction path for selected tip heights. Figure 2(c) shows the case when the tip is positioned close to the top site, where the CO molecule is initially adsorbed ($x/d = 0.3$). As discussed above, CO adsorption in the bridge configuration is energetically preferred for small tip-sample distances. However, the reaction pathway calculations [Fig. 2(c)] show that at the vertical tip position where the energies of the two states become comparable ($z_{\text{cal}} = 125$ pm), a spontaneous transition of the CO molecule on the top site to the bridge site is prevented owing to the existence of an energy barrier between the states. Notably, in our experiment, the sensor oscillated with a peak-to-peak amplitude of $2A = 40$ pm between its lower and upper turnaround points. If the tip oscillates around $z_{\text{cal}} = 125$ pm, then the barrier disappears when the tip is close to the lower turnaround point ($z_{\text{cal}} = 110$ pm), promoting the transition of CO to the bridge site. Conversely, when the tip retracts from the sample toward its upper turnaround point (e.g., $z_{\text{cal}} = 140$ pm), CO adsorption in the top site configuration becomes energetically most favorable. If, as in this case, a small energy barrier remains between the two configurations, the transition back to the top site does not necessarily coincide with the oscillation cycle. Assuming that the barrier height is ~ 10 meV from $z = 135$ to 145 pm, the period of an oscillation is 19 μs , the attempt rate of a laterally vibrated CO molecule is 1 THz (~ 4 meV) and the temperature is 4.4 K, the transition probability is estimated by the Arrhenius equation to be $\sim 2 \times 10^{-5}$ for one oscillation

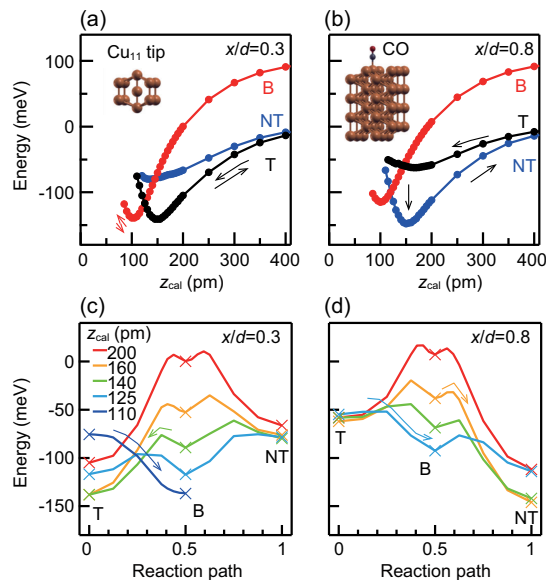


FIG. 2. (a) Theoretical potential energy between the Cu_{11} tip [inset of (a)] on $x/d = 0.3$ and CO on Cu(110) [inset of (b)] as a function of the vertical tip position (z_{cal}). The cases for CO on top (T), bridge (B), and neighboring top (NT) sites are depicted by black, red, and blue lines, respectively. (b) Same as (a) but for the tip over $x/d = 0.8$. (c) Calculated reaction pathways for CO from one top site (0.0) to the next top site (1.0) via bridge configuration (0.5) for a fixed Cu_{11} tip over $x/d = 0.3$. The cross marks correspond to CO in top (T), bridge (B), and neighboring top (NT) configurations, respectively. (d) Same as (c) but for the tip over $x/d = 0.8$.

cycle. Although this estimate is very sensitive to the actual tip height, it is reasonable to expect that the CO molecule will eventually return to the top site around the upper turnaround point of the tip. The above discussion implies that the top-to-bridge and the bridge-to-top manipulations occur at different tip heights, which is the origin of a hysteresis essential for the observation of energy dissipation.

Manipulation to neighboring top site.—The situation changes drastically when the tip is laterally positioned beyond the bridge site ($x/d > 0.5$). In this case, CO adsorption on the neighboring top site needs to be considered, because this conformation becomes more stable than the initial top site [Fig. 2(b)]. However, with the tip far away from the surface, manipulation between the two top sites is prevented owing to the larger energy barrier along the reaction path. The barrier height is approximately determined by the potential energy of the CO molecule adsorbed on the bridge site [$z_{\text{cal}} = 200$ pm in Fig. 2(d)]. When the tip approaches sufficiently close to CO, the manipulation from top to bridge is induced ($z_{\text{cal}} = 125$ pm), similarly to the case for $x/d < 0.5$. However, when the tip retracts from the molecule, the barrier from the bridge to neighboring top decreases ($z_{\text{cal}} = 160$ pm), which eventually results in the manipulation to the neighboring top site. This transition occurs

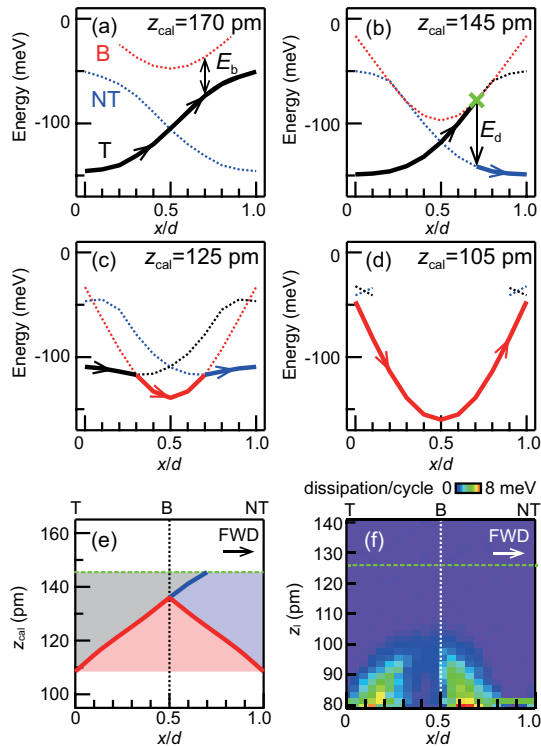


FIG. 3. (a) Calculated potential energy between the Cu_{11} tip and CO as a function of lateral tip position (at a constant tip height of 170 pm) for CO in top (T), bridge (B), and neighboring top (NT) configurations. The thick path represents the CO configuration during the lateral tip scan. (b)–(d) Same as (a) but for tip heights: (b) 145 pm, (c) 125 pm, and (d) 105 pm. (e) Calculated CO configuration as a function of tip height and lateral position during the forward tip scan. The gray, light red, and light blue regions represent CO in top (T), bridge (B), and neighboring top (NT) sites, respectively. The thick lines indicate the transition points. (f) Energy dissipation per cycle of the vertically oscillating tip, experimentally measured during the lateral CO dragging. In (e) and (f), the onset of dragging is indicated by the dashed green line.

only once for repeated approach and retraction of the tip, because CO on the neighboring top site is always more stable than that on the initial top site at this lateral tip position in the attractive force regime. As the CO molecule is manipulated only once, no energy dissipation can be observed in a time-averaged experiment [gray arrow for $x/d = 0.63$ in Fig. 1(g)].

CO manipulation by lateral tip motion.—The above scenario also explains the lateral manipulation process. Figures 3(a)–3(d) show the theoretical potential energies between tip and CO adsorbed on three different sites (top, bridge, and neighboring top) for four selected tip heights, where the tip (initially located over the top site at $x/d = 0$) is swept toward the neighboring top site at $x/d = 1$. Moreover, CO is initially adsorbed also on the top site at $x/d = 0$. For simplicity, we may consider that the transition of the CO molecule between top and bridge configurations occurs

spontaneously when their energies become equal (vanishing barrier). For large tip-sample distances [Fig. 3(a)], when the tip moves beyond the bridge site ($x/d > 0.5$), the energy of CO on the neighboring top site (blue) becomes lower than that on the top site (black). However, this manipulation is prevented owing to the presence of an energy barrier (E_b) as described for Fig. 2(d). This situation is changed by lowering the tip height, as shown in Fig. 3(b), where the black and red curves intersect around $x/d \sim 0.7$; CO can now be manipulated to the bridge site, resulting in a further manipulation to the neighboring top site [see Fig. 2(d)]. When the tip-sample distance decreases further [Fig. 3(c)], the black and red curves already intersect before the tip laterally approaches the bridge site. In this case, the CO molecule is first manipulated to the bridge site, where it stays until the red curve intersects with the blue curve, and the molecule is manipulated to the neighboring top site. Furthermore, if the tip height becomes very small [Fig. 3(d)], then only the bridge site is available for CO, indicating that no manipulation can take place.

The aforementioned processes are summarized in Fig. 3(e) for the forward scan. The regions depicted by gray, light blue, and light red areas correspond to CO adsorbed on the top, neighboring top, and bridge site, respectively. During the initial manipulation, involving the transition across the blue line in Fig. 3(e), we do not expect any energy dissipation as the CO molecule is manipulated only once from one top site to the next. When moving deeper into the contact regime, a considerable energy dissipation is expected for the manipulation across the red line, where transitions occur between the top and bridge sites correlated with the vertical tip oscillations. The transitions across the red line initially appear over the bridge site, and then split into two lateral positions when the tip height decreases. As evident from Fig. 3(f), these qualitative features of the dissipation were experimentally resolved during CO dragging (see Ref. [34] for details), thereby substantiating the microscopic picture of the manipulation steps.

Static and dynamic friction.—Our theoretical investigations provide further insights into both static and dynamic friction for the manipulation. In Fig. 3(b), the slope of the black line at the green cross corresponds to a static friction force (F_s) [33]. On the other hand, a dynamic friction force (F_d) can be considered as a force to keep an object in motion. Considering that its origin is the sequential energy dissipation process that occurs during the motion, F_d can be estimated by dividing the energy dissipation by the periodic distance of the manipulation. In the case of Fig. 3(b), the former corresponds to the energy difference between the black and blue lines at $x/d \sim 0.7$, marked as E_d , and the latter corresponds to the distance between the nearest neighboring Cu atoms (d). Using these estimates as a function of the tip height we find that the dynamic friction force is 10%–44% of the static friction force [34],

consistent with the empirical law for macroscopic systems [1,2].

Conclusions.—We have revealed the role of an intermediate state in the dynamics and energy dissipation during CO manipulation on a Cu(110) surface—the CO bridge site adsorption is enabled when the tip is brought close to the surface. Similar results are obtained using a different substrate (Cu(111)) [34], indicating the generality of intermediate states in manipulation pathways. The proposed mechanism may therefore also explain related manipulation studies with energy dissipation [19], including those for larger molecules such as perylenetetracarboxylic dianhydride [21]. In the future, the temperature dependence of dissipation processes could be analyzed, because at elevated temperatures the thermal energy helps the adsorbate to overcome barriers, thereby reducing energy dissipation. However, the controlled manipulation process with a tip may be challenging to separate from thermal diffusion processes at elevated temperatures. The balance between hysteretic effects in the energy landscape and thermal energy should be the key to control friction at the atomic scale at sufficiently low temperatures.

The authors thank Robert W. Carpick, Enrico Gnecco, Ferdinand Huber, Takashi Kumagai, Sonia Matencio, Daniel Meuer, Masao Obata, Hiroshi Okuyama, Magnus Paulsson, Angelo Peronio, Bo Persson, Jascha Repp, Akitoshi Shiotari, Toshiki Sugimoto, and Jay Weymouth for their valuable inputs on this research. This study was partially supported by funding from Deutsche Forschungsgemeinschaft (project No. CRC 1277, project A02), by JSPS KAKENHI Grants [No. 16K04959] [No. 16KK0096] [No. 20K05320] the European Union's Horizon 2020 program (Grant No. 863098) and by Spanish MCIN/AEI/10.13039/501100011033 Grant No. PID2020–115406GB-I00. N.O. appreciates University of Regensburg for the opportunity to conduct this study as a visiting professor.

*okabayashi@staff.kanazawa-u.ac.jp

†thomas_frederiksen@ehu.eus

‡franz.giessibl@ur.de

- [1] B. N. J. Persson, *Sliding Friction: Physical Principles and Applications* (Springer, New York, 2000).
- [2] A. Vanossi, N. Manini, M. Urbakh, S. Zapperi, and E. Tosatti, Colloquium: Modeling friction: From nanoscale to mesoscale, *Rev. Mod. Phys.* **85**, 529 (2013).
- [3] J. Y. Park and M. Salmeron, Fundamental aspects of energy dissipation in friction, *Chem. Rev.* **114**, 677 (2014).
- [4] R. Pawlak, S. Kawai, T. Meier, T. Glatzel, A. Baratoff, and E. Meyer, Single-molecule manipulation experiments to explore friction and adhesion, *J. Phys. D* **50**, 113003 (2017).
- [5] L. Gross, Recent advances in submolecular resolution with scanning probe microscopy, *Nat. Chem.* **3**, 273 (2011).
- [6] K. Bian, C. Gerber, A. J. Heinrich, D. J. Müller, S. Scheuring, and J. Ying, Scanning probe microscopy, *Nat. Rev. Methods Primers* **1**, 36 (2021).
- [7] E. Gnecco, R. Bennewitz, T. Gyalog, C. Loppacher, M. Bammerlin, E. Meyer, and H. J. Guntherodt, Velocity Dependence of Atomic Friction, *Phys. Rev. Lett.* **84**, 1172 (2000).
- [8] L. N. Kantorovich and T. Trevethan, General Theory of Microscopic Dynamical Response in Surface Probe Microscopy: From Imaging to Dissipation, *Phys. Rev. Lett.* **93**, 236102 (2004).
- [9] N. Oyabu, P. Pou, Y. Sugimoto, P. Jelinek, M. Abe, S. Morita, R. Perez, and O. Custance, Single Atomic Contact Adhesion and Dissipation in Dynamic Force Microscopy, *Phys. Rev. Lett.* **96**, 106101 (2006).
- [10] Y. F. Mo, K. T. Turner, and I. Szlufarska, Friction laws at the nanoscale, *Nature (London)* **457**, 1116 (2009).
- [11] Q. Li, T. E. Tullis, D. Goldsby, and R. W. Carpick, Frictional ageing from interfacial bonding and the origins of rate and state friction, *Nature (London)* **480**, 233 (2011).
- [12] S. Kawai, A. Benassi, E. Gnecco, H. Sode, R. Pawlak, X. L. Feng, K. Müllen, D. Passerone, C. A. Pignedoli, P. Ruffieux, R. Fasel, and E. Meyer, Superlubricity of graphene nanoribbons on gold surfaces, *Science* **351**, 957 (2016).
- [13] R. Pawlak, W. G. Ouyang, A. E. Filippov, L. Kalikhman-Razvozzov, S. Kawai, T. Glatzel, E. Gnecco, A. Baratoff, Q. S. Zheng, O. Hod, M. Urbakh, and E. Meyer, Single-molecule tribology: Force microscopy manipulation of a porphyrin derivative on a copper surface, *ACS Nano* **10**, 713 (2016).
- [14] A. J. Weymouth, E. Riegel, O. Gretz, and F. J. Giessibl, Strumming a Single Chemical Bond, *Phys. Rev. Lett.* **124**, 196101 (2020).
- [15] D. M. Eigler and E. K. Schweizer, Positioning single atoms with a scanning tunneling microscope, *Nature (London)* **344**, 524 (1990).
- [16] L. Bartels, G. Meyer, and K. H. Rieder, Basic Steps of Lateral Manipulation of Single Atoms and Diatomic Clusters with a Scanning Tunneling Microscope Tip, *Phys. Rev. Lett.* **79**, 697 (1997).
- [17] A. Kühnle, G. Meyer, S. W. Hla, and K. H. Rieder, Understanding atom movement during lateral manipulation with the STM tip using a simple simulation method, *Surf. Sci.* **499**, 15 (2002).
- [18] J. A. Stroscio and R. J. Celotta, Controlling the dynamics of a single atom in lateral atom manipulation, *Science* **306**, 242 (2004).
- [19] M. Ternes, C. P. Lutz, C. F. Hirjibehedin, F. J. Giessibl, and A. J. Heinrich, The force needed to move an atom on a surface, *Science* **319**, 1066 (2008).
- [20] B. Wolter, Y. Yoshida, A. Kubetzka, S. W. Hla, K. von Bergmann, and R. Wiesendanger, Spin Friction Observed on the Atomic Scale, *Phys. Rev. Lett.* **109**, 116102 (2012).
- [21] G. Langewisch, J. Falter, H. Fuchs, and A. Schirmeisen, Forces during the Controlled Displacement of Organic Molecules, *Phys. Rev. Lett.* **110**, 036101 (2013).
- [22] M. Emmrich, M. Schneiderbauer, F. Huber, A. J. Weymouth, N. Okabayashi, and F. J. Giessibl, Force Field Analysis Suggests a Lowering of Diffusion Barriers in Atomic Manipulation Due to Presence of STM Tip, *Phys. Rev. Lett.* **114**, 146101 (2015).

- [23] D. Yesilpinar, B. S. Lammers, A. Timmer, Z. X. Hu, W. Ji, S. Amirjalayer, H. Fuchs, and H. Monig, Mechanical and chemical interactions in atomically defined contacts, *Small* **17**, 2101637 (2021).
- [24] M. F. Crommie, C. P. Lutz, and D. M. Eigler, Confinement of electrons to quantum corrals on a metal-surface, *Science* **262**, 218 (1993).
- [25] A. J. Heinrich, C. P. Lutz, J. A. Gupta, and D. M. Eigler, Molecule cascades, *Science* **298**, 1381 (2002).
- [26] K. K. Gomes, W. Mar, W. Ko, F. Guinea, and H. C. Manoharan, Designer Dirac fermions and topological phases in molecular graphene, *Nature (London)* **483**, 306 (2012).
- [27] J. T. Yates, Chemisorption on surfaces—an historical look at a representative adsorbate: carbon-monoxide, *Surf. Sci.* **299**, 731 (1994).
- [28] F. J. Giessibl, The qPlus sensor, a powerful core for the atomic force microscope, *Rev. Sci. Instrum.* **90**, 011101 (2019).
- [29] J. E. Sader and S. P. Jarvis, Accurate formulas for interaction force and energy in frequency modulation force spectroscopy, *Appl. Phys. Lett.* **84**, 1801 (2004).
- [30] G. Kresse and J. Furthmüller, Efficient iterative schemes for *ab initio* total-energy calculations using a plane-wave basis set, *Phys. Rev. B* **54**, 11169 (1996).
- [31] J. Klimeš, D. R. Bowler, and A. Michaelides, Chemical accuracy for the van der Waals density functional, *J. Phys. Condens. Matter* **22**, 022201 (2010).
- [32] G. Mills, H. Jónsson, and G. K. Schenter, Reversible work transition-state theory—application to dissociative adsorption of hydrogen, *Surf. Sci.* **324**, 305 (1995).
- [33] See Supplemental Material at <http://link.aps.org/supplemental/10.1103/PhysRevLett.131.148001> for additional information on the tip height definition, frequency shift and dissipation measurements, and the static friction comparison between experiment and theory. The simulation input and output dataset is freely available for download at DOI: [10.5281/zenodo.8261814](https://doi.org/10.5281/zenodo.8261814).
- [34] N. Okabayashi, T. Frederiksen, A. Liebig, and F. J. Giessibl, companion paper, Energy dissipation of a carbon monoxide molecule manipulated using a metallic tip on copper surfaces, *Phys. Rev. B* **108**, 165401 (2023).